MICROBIOLOGY

A viral scaffolding protein triggers portal ring oligomerization and incorporation during procapsid assembly

Tina Motwani,[1] Ravi K. Lokareddy,[2] Carmen A. Dunbar,[3] Juliana R. Cortines,[1]* Martin F. Jarrold,[3] Gino Cingolani,[2,4] Carolyn M. Teschke[1,5†]

Most double-stranded DNA viruses package genetic material into empty precursor capsids (or procapsids) through a dodecameric portal protein complex that occupies 1 of the 12 vertices of the icosahedral lattice. Inhibiting incorporation of the portal complex prevents the formation of infectious virions, making this step an excellent target for antiviral drugs. The mechanism by which a sole portal assembly is selectively incorporated at the special vertex is unclear. We recently showed that, as part of the DNA packaging process for bacteriophage P22, the dodecameric procapsid portal changes conformation to a mature virion state. We report that preformed dodecameric rings of P22 portal protein, as opposed to portal monomers, incorporate into nascent procapsids, with preference for the procapsid portal conformation. Finally, a novel role for P22 scaffolding protein in triggering portal ring formation from portal monomers is elucidated and validated by incorporating de novo assembled portal rings into procapsids.

INTRODUCTION

Tailed double-stranded DNA (dsDNA) bacteriophages and herpesviruses encapsulate their genome into preformed icosahedral protein shells. Assembly of these viruses begins with the formation of a metastable precursor structure known as a procapsid (PC), prohead, or prehead (*1*, *2*). Chemically identical coat protein (CP) subunits are organized into hexameric and pentameric configurations in the PC in accordance with Caspar and Klug's theory of quasi-equivalence (*3*). A single vertex of the icosahedron is occupied by a ring-shaped oligomer of a "connector" or "portal protein" (*4*). The portal protein complex functions as a conduit for dsDNA translocation both into and out of the capsid during assembly and infection (*4*). This function is made possible by its ability to form a docking site for the DNA packaging terminase, plug proteins, and tail proteins in bacteriophages (*4*–*8*). Thus, by inhibiting incorporation of the portal complex, the formation of infectious virions could be prevented, making portal protein incorporation a possible drug target for herpesviruses.

Atomic structures of the portal protein complex from *Podoviridae* (P22 and Φ29), *Siphoviridae* (SPP1), and *Myoviridae* (T4) tailed bacteriophages have been determined (*9*–*12*). Comparison of these structures highlights the similarities in oligomeric complexes and well-conserved domain structures, despite low sequence similarity (*12*). In addition, herpes simplex virus type 1 (HSV-1) portal protein has a strikingly similar morphology to the portals of dsDNA bacteriophage, as determined by reconstruction of cryo-electron micrographs (*13*–*16*). Our recent structural studies indicate that the portal protein of bacteriophage P22 exists in at least two distinct dodecameric conformations, depending on the state of capsid maturation. The portal protein complex (~0.96 MDa) in PCs (referred to as "PC portal") forms an asymmetric ring with an unfolded barrel domain (Fig. 1A) (*17*), whereas the portal in mature virions (referred to as "MV portal") folds into a ring of 12 conformationally identical subunits, symmetrically arranged around a central channel (Fig. 1B) (*10*). The C-terminal residues (603 to 725) form an elongated helical barrel extending inside the virion, a feature unique to P22-like bacteriophages (*18*). Molecular modeling studies reveal that packaging of dsDNA into the PC triggers conformational changes in the PC portal to acquire the symmetric conformation observed in the MV portal (*17*).

The well-characterized assembly pathway of the bacteriophage P22 makes it an ideal model system to study the mechanism of portal protein incorporation (*19*). During P22 morphogenesis, scaffolding protein (SP) (60 to 300 molecules) acts as an assembly chaperone, directing the polymerization of 415 molecules of CP, and is essential to the addition of the portal protein and several minor ejection proteins into a $T = 7$ icosahedral metastable PC (*1*, *6*, *7*, *20*–*23*). In P22, incorporation of a single portal ring is essential to viable virion formation and occurs with 95% efficiency in vivo (*24*). This high level of fidelity statistically rules out random incorporation and suggests that it occurs at a single step in the assembly process. Murialdo and Becker (*25*) were the first to propose that portal incorporation into dsDNA phage PCs is driven by a nucleation mechanism, where nucleation is the rate-limiting step in the assembly, and the presence of portal protein enhances this initiation. However, for P22, there is no difference in assembly kinetics in vivo in the presence or absence of portal protein, suggesting that it is not the initiator of assembly (*6*). Various other mechanisms of portal protein integration have been suggested and include incorporation during the final step of assembly (*26*, *27*), at an intermediate step (*27*), or through an obligate portal protein/mRNA interaction (*28*); however, there is little experimental evidence for any of these hypotheses.

To dissect the mechanism of portal incorporation into PCs at the molecular level, an in vitro system that is able to detect portal incorporation into PC is essential. In vitro portal protein incorporation during assembly of PC has been reported only for HSV-1 and bacteriophage Φ29. In HSV-1, the portal protein is incorporated in an early assembly step (*29*). The portal complex (connector protein) of bacteriophage Φ29 can be incorporated into PCs during in vitro assembly in the presence of a molecular crowding agent (*30*). The yield and rate of Φ29 assembly

[1]Department of Molecular and Cell Biology, University of Connecticut, 91 North Eagleville Road, Storrs, CT 06269, USA. [2]Department of Biochemistry and Molecular Biology, Thomas Jefferson University, 233 South 10th Street, Philadelphia, PA 19107, USA. [3]Department of Chemistry, Indiana University, 800 East Kirkwood Avenue, Bloomington, IN 47405, USA. [4]Institute of Biomembranes and Bioenergetics, National Research Council, Via Amendola 165/A, 70126 Bari, Italy. [5]Department of Chemistry, University of Connecticut, Storrs, CT 06269, USA.
*Present address: Departamento de Virologia, Instituto de Microbiologia Paulo de Góes, Universidade Federal do Rio de Janeiro, CEP 21941-902, Rio de Janeiro, Brazil.
†Corresponding author. Email: carolyn.teschke@uconn.edu

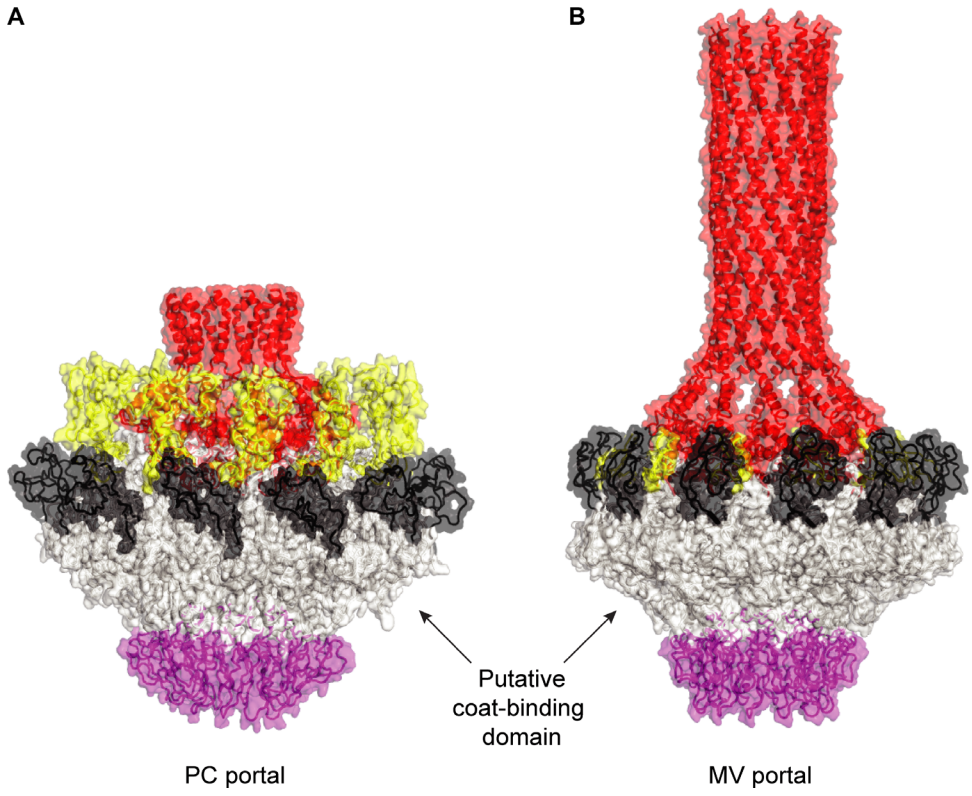

Fig. 1. Structural comparison of the PC versus MV portal protein structures. Ribbon diagrams of P22 portal protein ring in PC (**A**) and MV (**B**) conformations. The portal oligomer is colored gray, with stalk, trigger loop, hammer loop, and barrel domain colored magenta, black, yellow, and red, respectively. Arrows indicate the coat-binding region present in the PC and MV portal protein structures.

increase in the presence of the connector protein, as expected, because it serves as the assembly nucleator. In both studies, the dodecameric (12-mer) portal complex, and not the monomeric portal subunits, was used for the in vitro reactions.

Here, we have investigated the mechanism of portal protein incorporation in P22 PCs, testing both the PC and MV conformational states of portal dodecamers and monomers as substrates in assembly. We found that the PC portal is favored, and monomers are not incorporated. We also discovered an additional key role for SP: activating portal ring formation from monomers before complex incorporation into PCs.

RESULTS

In vitro assembled PC and MV portals are exclusively dodecameric

To investigate the mechanism of portal protein incorporation into P22 PCs, we first isolated the P22 portal protein in its PC and MV conformations following established purification protocols (*10*, *17*, *23*). Briefly, to assemble PC portal, portal monomers (PMs) were purified in low salt, at physiological pH, and assembled into oligomers by ultrafiltration concentration, followed by purification by size exclusion chromatography (SEC) (*17*). MV portal was purified by subjecting highly concentrated PMs to heat shock in the presence of EDTA that selectively promotes maturation to the MV conformation, followed by ultracentrifugation to pellet contaminating oligomers and unassembled monomers (*10*, *23*). Consistent with a published report by Lokareddy *et al.* (*17*), PC portal rings had high affinity for L-terminase, whereas the MV portal had negligible affinity for the packaging motor. We then labeled preassembled PC and MV portal rings and PMs with Alexa Fluor 488 (AF488) sulfodichlorophenol (5-SDP) ester dye to use in our in vitro incorporation assays. The portal proteins needed to be fluorescently labeled, because there are no antiportal antibodies that bind P22 portal protein in PC, and because of the need to increase the sensitivity of our assays. The labeled portal rings (PC or MV) and PM will be henceforth referred to as AF488 PC portal, AF488 MV portal, or AF488 PM.

We follow the elution of PCs, PC portal, or MV portal from a Superose 6 Increase size exclusion column to distinguish the various proteins and complexes. Both unlabeled PC (Fig. 2A) and MV portal (Fig. 2B) rings elute as a single, well-resolved peak centered at 11.90 and 12.0 ml, respectively. Because the MV portal does not have a histidine tag, we expected that it should be slightly retained compared to PC portal. PCs eluted in the void volume, at 8.80 ml. The apparent molecular weights (MWs) of PC and MV portals were consistent with previously published reports, suggesting complete oligomerization of portal proteins (*31*, *32*). AF488 PC portal and AF488 MV portal eluted at comparable volumes as their unlabeled counterparts (Fig. 2, A and B, bottom panel, respectively), indicating that labeling of portal rings with AF488 5-SDP ester does not alter the oligomeric state of the proteins.

Previous studies showed that in vitro purified and assembled P22 portal protein can form undecamers (11-mer) and dodecamers (12-mer) in a ratio of approximately 2:1 (*23*, *33*). Using charge detection mass spectrometry (CDMS) and native gel electrophoresis, we confirmed the oligomeric state of our in vitro assembled PC and MV portal (unlabeled and AF488-labeled) rings. In CDMS, the mass-to-charge ratio (m/z) and charge of individual ions are measured simultaneously, yielding the mass of each ion (*34*–*36*). Figure 2 shows the mass spectra of unlabeled and

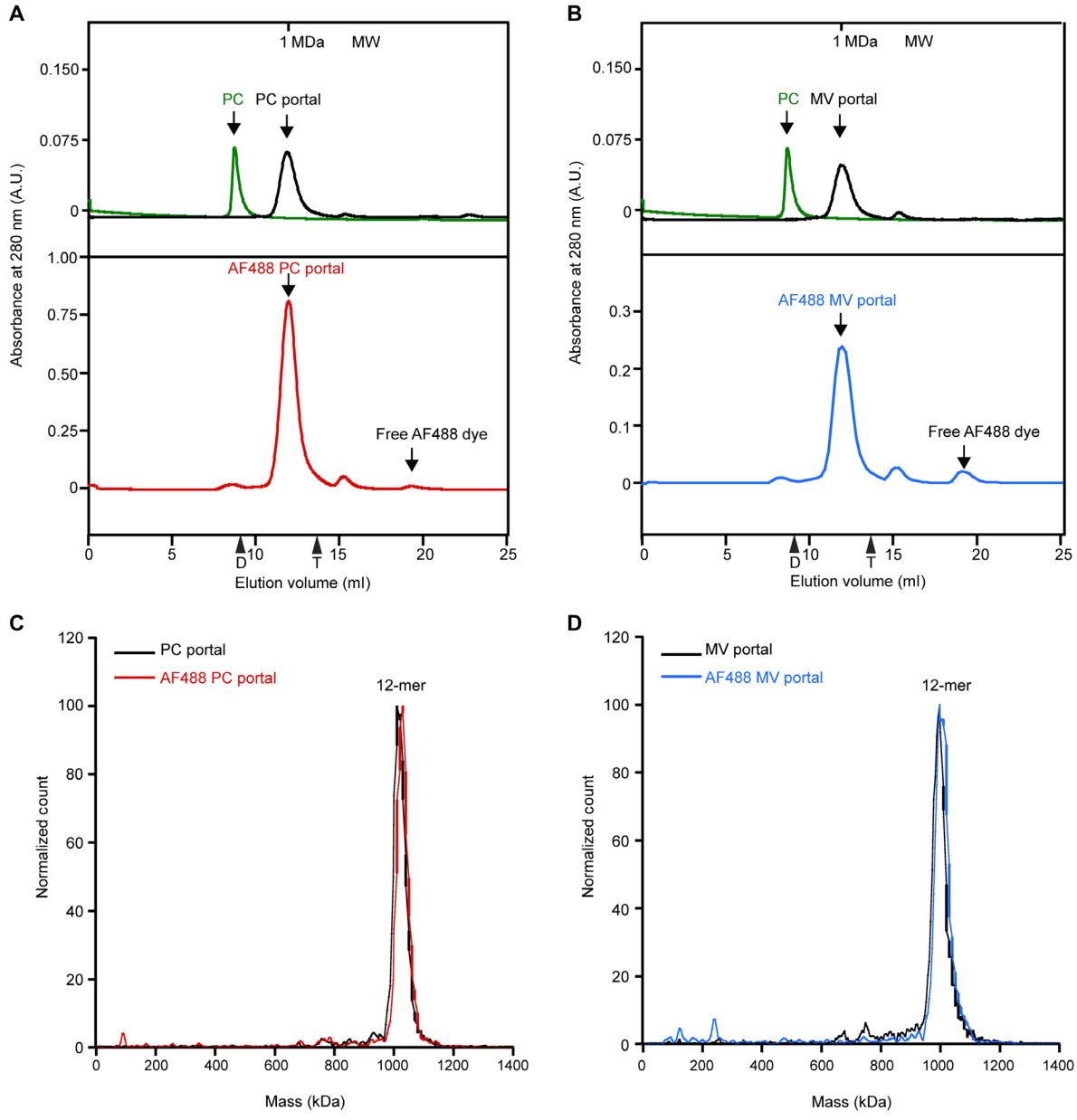

Fig. 2. In vitro assembled PC and MV portals are exclusively dodecameric. (**A** and **B**) Top: Elution profiles of unlabeled PCs and PC portal (A) or MV portal (B). Bottom: Elution profiles of AF488-labeled PC portal (AF488 PC portal) or MV portal (AF488 MV portal) applied to a Superose 6 gel filtration column. The MW was determined on the basis of the calibration standards that are marked along the top *x* axis. The arrowheads on the bottom *x* axis indicate the location of the MW markers (D, dextran blue, 2000 kDa; T, thyroglobulin, 669 kDa). A.U., arbitrary units. Mass spectra of unlabeled and labeled PC portal (**C**) and MV portal (**D**) measured by CDMS. PC, MV, and AF488-labeled portal samples were buffer-exchanged using SEC into 100 mM ammonium acetate. The quadrupole mass filter was set to discard ions with *m/z* values below 4000 Da. The measured masses were binned using 5000-Da bins.

AF488-labeled PC portal (Fig. 2C) and MV portal (Fig. 2D). For both the PC and MV portals, the 12-mer peak dominates the spectrum; there were only a few ions detected at lower mass, which range from 11- to 8-mer. The measured mass of the 12-mer peaks of both the PC and MV portals (unlabeled) determined by fitting a Gaussian to the measured peak and taking the center, along with the theoretical masses (obtained from the sequences), are shown in Table 1. The measured masses are averages of multiple preparations, and the uncertainties are ±1 SD. The measured masses are expected to be up to around 1% larger than the theoretical masses because of incomplete removal of solvent. For the MV portal, the difference is 0.4%, whereas for the PC portal, it is 2.4%. Nevertheless, the CDMS results indicate that the dodecamer is the dominant species for both the PC and MV portals. The measured masses of AF488 PC portal and AF488 MV portal were comparable to their unlabeled counterparts. Additionally, the unlabeled and labeled PC and MV portals migrate to the 1-MDa position on blue native bis-tris 4 to 16% gels, again demonstrating oligomerization of portal protein monomer (~83.8 kDa for His-tagged PC portal or ~82.7 kDa for untagged MV portal) into 12-mer dodecameric rings (fig. S1). Together, our results indicate that the in vitro assembled portal rings (PC portal or MV portal) are primarily dodecameric.

Portal rings can be assembled into PCs in vitro

Previous studies using bacteriophage Φ29 and herpes virus demonstrated incorporation of portal 12-mer rings into PC in vitro (*29*, *30*). We took advantage of the recently characterized different conformational states of the P22 portal complex (*10*, *17*) and tested which of the preassembled dodecameric portal rings species, PC portal or MV portal, were competent for assembly. We hypothesized that the asymmetric PC portal would be the active species and be more efficiently incorporated into P22 PC compared to the symmetric MV portal (*10*, *17*). On the basis of the in vitro assay outlined in Fig. 3, the assembly reactions as described in Table 2 were performed. Briefly, purified SP and AF488 PC portal or AF488 MV portal (Rx1) were preincubated for 4 hours at room temperature (RT). Using this preincubation time, maximal portal protein incorporation was achieved during PC assembly. PC assembly was initiated by the addition of CP monomers and allowed to reach completion (4 hours). Completion occurs when the CP concentration drops below its critical concentration and is unable to support further PC polymerization (*37*). In our in vitro assembly experiments, SP is in excess and does not limit the reaction (*37*). In these experiments, the reactions are complete within 60 min under all conditions. After the reactions were completed, the assembled products were separated from the input proteins using SEC, and the PC peak was analyzed by SDS–polyacrylamide gel electrophoresis (PAGE) to determine portal protein incorporation. As a negative control, we used empty PC shells in place of the CP monomers because portal protein is not incorporated into preassembled PC-like particles (PLPs) (*27*, *38*). The shells were incubated with AF488 PC portal or AF488 MV portal (Rx2) and analyzed as described above. In addition, we also analyzed AF488-labeled PC portal or MV portal alone (Rx3) incubated in buffer at RT.

The elution profiles of assembly reactions carried out with CP and SP, plus AF488 PC portal or AF488 MV portal (Rx1), are shown in Fig. 4 (A and D, respectively). The elution profiles of the mock reactions using empty PC shells, plus AF488 PC portal or AF488 MV portal (Rx2), along with AF488 PC portal or MV portal alone (Rx3), are also shown. The black arrowhead indicates the elution volume of the in vitro assembled PC (see Fig. 2). Three fractions with the highest absorbance were taken from the PC peak of Rx1, Rx2, and Rx3 to be analyzed by SDS-PAGE. The presence of AF488-labeled portal protein in the PC fractions was visualized using a PharosFx Plus Molecular Imager at an excitation wavelength of 488 nm (Fig. 4, B or E, top gel), followed by silver staining (Fig. 4, B or E, bottom gel). Consistent with our hypothesis, the AF488-labeled preassembled dodecameric PC portal (Fig. 4B, Rx1) was incorporated into in vitro assembled PCs. The portal protein did not elute in the PC peak in our mock reactions (Fig. 4B, Rx2 and Rx3). We also saw incorporation of AF488 MV portal (Fig. 4E, Rx1), albeit with lower efficiency than with AF488 PC portal rings. We believe that MV portal is incorporated because the coat-binding region of PC and MV portals (Figs. 1 and 9) is very similar.

As mentioned above, we observed no incorporation of either PC or MV portals in our mock reactions with empty PC shells, indicating that the portal protein does not interact nonspecifically with the surface of assembled PCs. To rule out the possibility of nonspecific association of PC or MV portal rings within the interior of the in vitro assembled PC, we performed assembly reactions where labeled portal rings were replaced with AF488-labeled ovalbumin. Ovalbumin should not be specifically incorporated but could be trapped on the interior of PC. No coelution of ovalbumin with the PC peak from the Superose 6 Increase column was observed (fig. S2B, Rx1). Instead, the AF488-labeled ovalbumin eluted along with the free CP and SP (fig. S2C, Rx1). Thus, our data are consistent with specific incorporation of preassembled dodecameric rings into in vitro assembled bacteriophage P22 PC.

Table 1. Mass of the PC and MV portals determined from CDMS spectra.

Sample	Theoretical mass of 12-mer (kDa)	Measured mass of 12-mer (kDa)*
PC portal	1005.6	1027 ± 0.009
MV portal	992.9	997.2 ± 0.004

*The measured masses were obtained by fitting a Gaussian to the measured peak and taking the center of the Gaussian. The mass difference observed between the PC and MV portals is due to the His tag bound to the PM. The uncertainties for the measured masses are ±1 SD for multiple measurements on different samples.

Electron micrographs of in vitro assembled PC with portal incorporated

The specific incorporation of portal protein in in vitro assembled PCs at a single vertex was confirmed by immunonegative stain transmission electron microscopy (TEM). Purified PC from the assembly and the

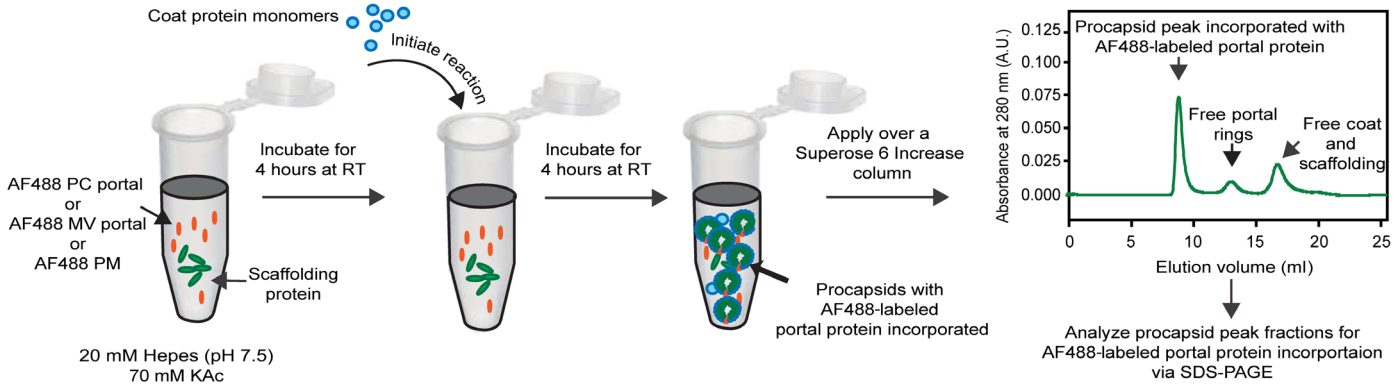

Fig. 3. Bacteriophage P22 in vitro assembly reaction. AF488 PC portal, AF488 MV portal, or AF488 PM were preincubated with SP in 20 mM Hepes (pH 7.5) and 70 mM potassium acetate (KAc) buffer for 4 hours at RT. The assembly reaction was initiated by the addition of CP monomers. After 4 hours, the assembly products were applied to a Superose 6 gel filtration column (GE Healthcare) to separate in vitro assembled PCs from unincorporated CP, SP, and labeled portal protein monomers or portal rings (PC portal or MV portal). The PC peak fractions were analyzed for AF488-labeled portal protein incorporation by SDS-PAGE.

Table 2. In vitro assembly reaction setup.

Reaction no.	Components of assembly reaction*	Concentration*
Rx1	SP	9 μM
	AF488 PM or AF488 PC portal or AF488 MV portal	1.1 μM
	Coat monomers	6.4 μM
Rx2	AF488 PM or AF488 PC portal or AF488 MV portal	1.1 μM
	Shells	3.2 μM
Rx3	AF488 PM or AF488 PC portal or AF488 MV portal	1.1 μM

*The components and the concentration of which each protein was added in the reaction are mentioned.

mock reactions with AF488 PC portal and AF488 MV portal (Fig. 4, A or D, black arrowheads) were absorbed to carbon-coated, 300-mesh copper grids. They were treated with primary antibody against AF488, followed by a secondary antibody conjugated with 10-nm colloidal gold beads, and negatively stained with uranyl acetate. Analysis of the micrographs revealed the presence of gold label at a single capsid vertex in PCs (<15 μm from the PC) assembled in the presence of AF488 PC portal (Fig. 4C) or AF488 MV portal (Fig. 4F). As shown in Table 3, the efficiency of portal protein incorporation into in vitro assembled PCs was 12% with AF488 PC portal and 6% with AF488 MV portal. Particles with two gold beads localized at different vertices were rarely observed. The negative control of empty PC shells incubated with labeled PC portal or MV portal (Fig. 4, C and F, respectively, and Table 3) showed only 0.5 to 1% incorporation efficiency. One percent to 2% of PCs displaying the immunogold bead at the center of the particle were included in our count, instead of the edge as depicted in Fig. 4 (C and F). This orientation was likely due to the PC landing with the portal complex down on the grid, resulting in the center positioning of the immunogold bead. The portal protein incorporation efficiency in our assembly reactions is comparable to the levels observed for bacteriophage Φ29, but lower than HSV-1 (*29*, *30*).

SP catalyzes portal ring oligomerization

We next tested whether PMs were active in assembly. We anticipated that monomers would not be incorporated; however, we saw incorporation of labeled PMs (AF488 PM) into PCs (Fig. 5, B and C, Rx1). This unexpected result (Fig. 5, Rx1) could be explained in two ways. First, the PMs could oligomerize into assembly-competent portal rings because of the incubation with phage proteins (CP or SP), which would subsequently be incorporated into PC. Second, PMs could be directly incorporated into PC during assembly, forming the dodecameric rings simultaneously with assembly.

To test the first hypothesis that PMs might be triggered to oligomerize and, as a consequence, be incorporated into nascent PCs, we incubated AF488 PM (1.1 μM) with either SP (9 μM) or CP (6.4 μM) for 4 hours at RT, followed by SEC of reaction product. The resulting fractions were analyzed by SDS-PAGE, and the presence of AF488-labeled portal rings or PMs was detected by fluorescence emission at 488 nm. In Fig. 6, we show that AF488 PM remains monomeric when incubated alone at RT, consistent with the published report that shows that in vitro P22 portal protein monomers are metastable and assemble into oligomers only at high concentration and with long incubation times (*31*). On the other hand, portal rings were observed when AF488 PM was incubated with SP, suggesting that SP can facilitate the formation of portal rings from PMs. We also observed that CP could catalyze the formation of portal rings, but with lower efficiency. To test whether the formation of portal rings from PMs specifically required a phage protein (SP or CP), we incubated AF488 PM with ovalbumin. We chose ovalbumin because it is around the same MW as coat and SPs. No rings were generated upon incubation with ovalbumin. In addition, incubation of AF488 PM with empty PC shells also had no effect on the oligomeric state of PMs. Together, our results indicate that SP, and to a much less extent CP, specifically triggers the formation of portal rings from PMs.

We further characterized the de novo assembled portal rings obtained in the presence of SP using sucrose gradient and TEM. We incubated unlabeled PM with SP at a final concentration of 16.5 and 135 μM, respectively, for 4 hours at RT. As controls, we individually incubated PM and SP and preassembled dodecameric portal rings in the buffer for 4 hours at RT. The equilibrated samples were each sedimented through a linear 5 to 20% sucrose gradient. The portal and SPs in the fractions were analyzed by SDS-PAGE and quantified by densitometry. As shown in Fig. 7A, we observe that individually PM and SP sediment at the top of the sucrose gradient. In contrast, when PM was incubated with SP, we observed a shift in both the SP and the portal protein migration down the gradient into higher sucrose concentrations and toward the position of the preassembled dodecameric portal rings, suggesting the formation of complexes larger than either PMs or SP. Analysis of fraction 14 of this sucrose gradient shows the presence of ring-like structures, similar in size and morphology to those of preassembled dodecameric portal rings (Fig. 7B). These ring-like structures were absent in fraction 14 of sucrose gradients where PM or SP was applied. Using CDMS, the oligomeric state of SP-catalyzed de novo portal rings from the monomer pool was determined and compared to the mass of PM (fig. S3). In this spectrum, the red line shows the mass distribution for the PM before the addition of SP, and the peak was centered around ~84 kDa. The black line shows the spectrum after the addition of SP. The black spectrum extends to a much higher mass (from 250 to 1500 kDa), and the resolution evident in the red spectrum is lost. The loss of resolution is consistent with the complex formation between the portal and SPs and results in the formation of heterogeneous portal protein oligomers, possibly larger than trimers (3-mer) and including assembled dodecameric rings (fig. S3). The interaction of SP with the assorted portal complexes likely contributes to the heterodispersity of the peaks and, at least, some higher mass complexes. Together, our data show that interaction between the PM and SP facilitates oligomerization of portal rings.

SP interacts with PMs, not with preassembled portal rings

Next, we investigated the interaction between SP and PMs (PM) or portal rings (PC and MV portals) by weak-affinity chromatography (*39*). With this technique, specific but reversible interactions between the two proteins can be qualitatively assessed (*37*). His-tagged PM or PC portal was bound to an immobilized metal affinity column (IMAC). The untagged MV portal was conjugated to *N*-hydroxysuccinimide (NHS)–agarose beads, as described in Materials and Methods. SP was then applied to the column. The retention of SP on the column is directly related to the strength of its binding to PM, PC portal, or MV portal; thus, an increase in elution volume is expected if SP interacts with PMs or rings. The

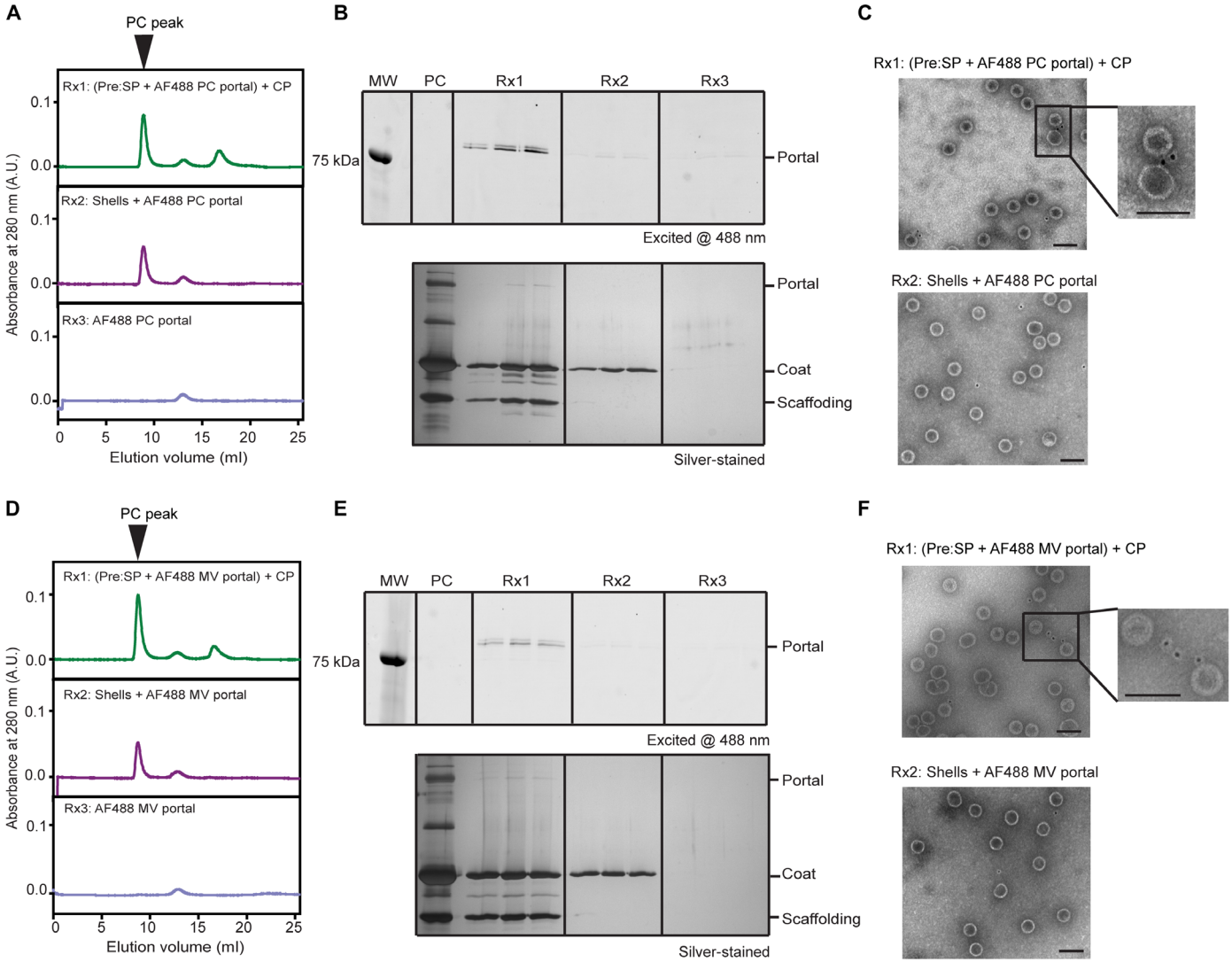

Fig. 4. In vitro, both PC and MV portals are incorporated into PCs. Superose 6 elution profiles of the assembly reactions (Rx1) of CP and SP with AF488 PC portal (**A**) or AF488 MV portal (**D**) are shown along with the elution profiles from the mock reactions with empty PC shells (Rx2) and AF488-labeled PC portal, or MV portal alone (Rx3). The black arrowhead indicates the elution volume of in vitro assembled PC peak from the column. Three fractions from the PC peak from Rx1, Rx2, and Rx3 were subjected to SDS-PAGE. MW standard (MW, lane 1) and unlabeled PC marker (PC, lane 2) are also shown. The presence of labeled PC portal (**B**) or MV portal (**E**) in the PC peaks was visualized using a PharosFx Plus Molecular Imager (top), followed by silver staining (bottom). Electron micrographs of in vitro assembled P22 PC (Rx1) and empty PC shells (Rx2) in the presence of AF488 PC portal (**C**) or MV portal (**F**). Insets show magnified views of particles boxed in (C) and (F), respectively. In these particles, the immunogold-labeled portal protein is seen at a single capsid vertex. Scale bars, 100 nm. Note that, in the magnified view of (F), only the bead near the PC in the bottom right would have been counted. The other two beads between the PC were >15 μm from the PC.

Table 3. In vitro assembled P22 PCs containing gold particles.

PC type*	Total number of PCs counted	Number of PCs with gold particles	%
(A) (Pre: SP + AF488 PC portal) + CP	954	114	12.0
(B) Shells + AF488 PC portal	1340	7	0.5
(C) (Pre: SP + AF488 MV portal) + CP	1000	64	6.4
(D) Shells + AF488 MV portal	739	6	0.8

*PCs or empty PC shells assembled in vitro in the presence of AF488 PC portal or AF488 MV portal.

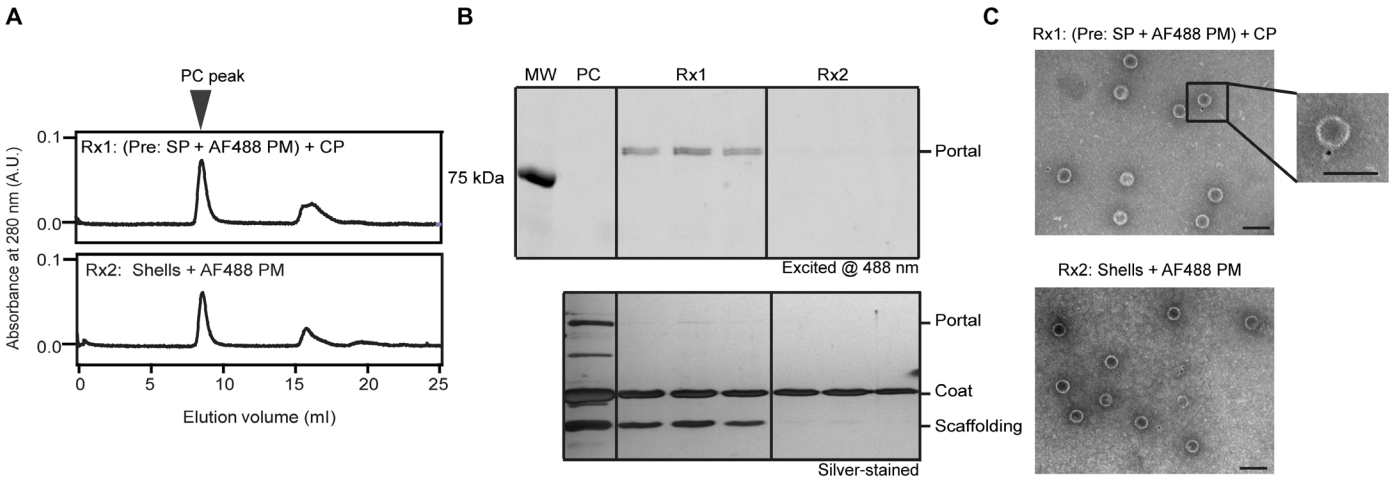

Fig. 5. De novo oligomerized portal rings are assembly-competent. (**A**) Superose 6 elution profiles of the assembly reactions of CP and SP with AF488 PM (Rx1), along with the elution profiles from the mock reactions, where empty PC shells are incubated with AF488 PM (Rx2). (**B**) The three fractions corresponding to the SEC-purified PC peak from Rx1 and Rx2 were subjected to SDS-PAGE. The presence of AF488-labeled portal protein was visualized using a PharosFx Plus Molecular Imager at an excitation wavelength of 488 nm (top), followed by silver staining (bottom). MW standard (MW, lane 1) and unlabeled PC marker (PC, lane 2) are also shown. (**C**) Electron micrographs of in vitro assembled P22 PCs (Rx1) and empty PC shells (Rx2) in the presence of AF488 PM. Insets show magnified views of particles boxed in (C). Scale bars, 100 nm.

interaction of CP with PMs or rings was also tested. The intrinsic tryptophan fluorescence of the proteins was used to monitor elution from the weak-affinity column. Ovalbumin was used as a negative control (*40*). Notably, SP has only one tryptophan, whereas CP has six, so SP fluorescence is low relative to CP.

The negative control, ovalbumin, eluted around 2 ml from each weak-affinity column, setting the standard elution volume for a noninteracting protein (Fig. 8, A to C). CP eluted at 2.25 ml, indicating very weak or negligible interaction with PMs (Fig. 8A) or preassembled portal rings (Fig. 8, B and C, respectively). SP eluted at 2.25 ml from the PC portal column and at 2.5 ml from the MV portal weak-affinity column, suggesting that SP interacts weakly with preassembled portal rings (Fig. 8, B and C, respectively). On the other hand, SP eluted as a very broad peak with a long tail, centered at 3.5 ml from the PM column, indicating that SP binds relatively strongly to PMs (Fig. 8A). We hypothesize that the SP interaction site with portal protein monomers becomes buried upon oligomerization, consistent with the low affinity of SP for the PC and MV portals. We propose that the interaction between SP and portal rings must be much weaker, possibly on the same order of magnitude as CP interaction with SP; otherwise, the assembly reaction could not proceed because the reactant proteins would be sequestered in the complex and not available for PC assembly. Our current experiments, however, cannot distinguish between the possibilities that the SP molecules used in the catalysis of portal ring formation are, or are not, the same molecules used to facilitate incorporation of the de novo assembled rings into PC. Nevertheless, these data support our hypothesis that SP interacts with PMs to catalyze the formation of portal rings, which are subsequently incorporated into PCs.

DISCUSSION

Encapsidation of genomes into preassembled PCs in dsDNA bacteriophages and herpesviruses occurs through a unique portal vertex. As was seen with the in vitro studies in HSV-1 and bacteriophage Φ29 (*29*, *30*), our results show that the portal protein of bacteriophage P22 preferentially gets incorporated into PCs as the preassembled dodecameric portal rings (PC and MV portals) rather than as PMs (Fig. 4). Contrary to our hypothesis that PC portal was likely to be the competent species for incorporation into P22 PC, we also saw incorporation of MV portal, although with a lower efficiency. The assembly of MV portal into PCs in vitro likely reflects a nonphysiological scenario. In vivo, MV portal will form only in the assembled virion as a result of DNA packaging by the large terminase (*17*). At the structural level, the major conformational changes between the PC and MV portals occur within the protein surface–exposed "trigger" loop (residues 226 to 277) that is part of the wing domain (Fig. 9, black curved arrow) (*17*). However, the stem and wing regions (residues 10 to 225 and 278 to 341) comprising the coat-binding regions that interact with CP in the capsid (*18*) do not undergo major conformational transitions between the two portal structures (Fig. 9, black box). Two-loop regions (residues 41 to 59 and 191 to 217), which are part of the putative coat-binding domain and interact with CP in PC (highlighted by the gray dashed circle in Fig. 9), do show conformational differences. We propose that these loops must be very dynamic and able to interact with CP in either portal conformation. The requirement to shift the loop present in the MV portal back to the PC portal conformation may explain the lower efficiency of incorporation. Alternatively, the loop may somewhat occlude interactions with CP and decrease the interaction affinity. Nevertheless, we conclude that, because the core of the putative coat interaction domain of both PC and MV portals is similar, both dodecameric portal ring conformations can be incorporated in vitro, albeit for MV portal this is an artifact of an in vitro system.

In HSV-1, the efficiency of portal protein incorporation into in vitro assembled PCs was 30 to 35% (*29*), whereas we observed that, for P22, the portal protein incorporation efficiency into PCs reached only 12%, comparable to the levels observed for bacteriophage Φ29 (Table 3) (*30*). The relatively low portal protein incorporation efficiency observed in our assembly reactions could be attributed to several reasons. First, AF488 dye on the portal rings is likely only partially accessible to the anti-AF488 primary antibody, decreasing the apparent yield. Second, our concentration of active portal rings is almost certainly lower than the input concentration, and we have no accurate way at this point to establish activity. Finally, other factors may play a role in portal complex incorporation during the in vivo P22 morphogenesis,

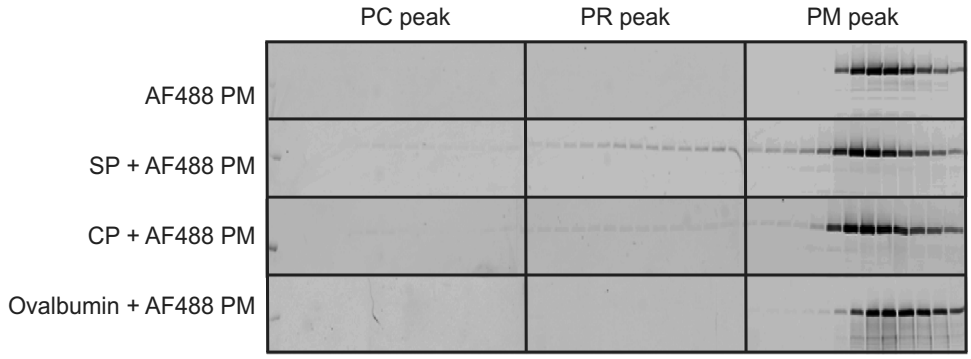

Fig. 6. SP acts as a "facilitator" of portal ring oligomerization. SP, CP, or ovalbumin was incubated with AF488 PM in 20 mM Hepes (pH 7.5) and 70 mM KAc buffer for 4 hours at RT. The reactions were applied over Superose 6 Increase column. The fractions harboring the PC, portal rings (PR), and PM peaks, 8 to 17.5 ml, were subjected to SDS-PAGE, and the presence of AF488-labeled portal rings or PMs in these fractions was visualized by PharosFx Plus Molecular Imager at an excitation wavelength of 488 nm.

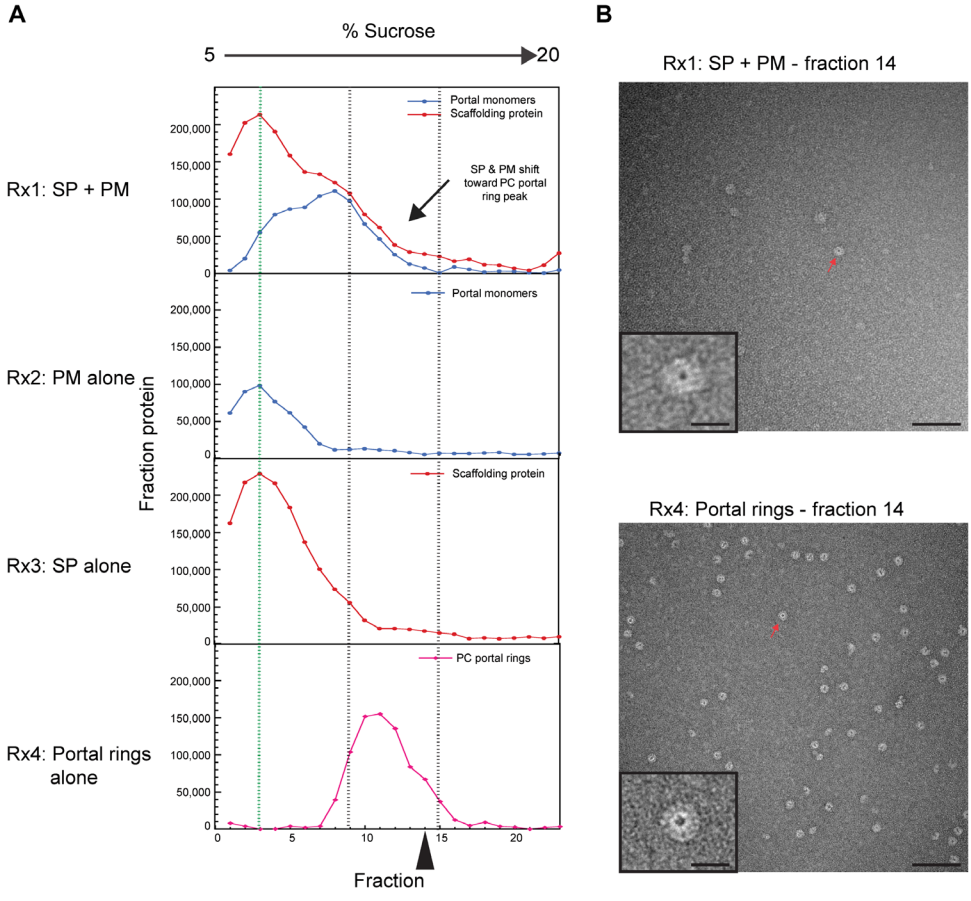

Fig. 7. De novo assembled portal rings analyzed by sucrose gradient and TEM. (**A**) Densitometry profile of de novo ring nucleation reaction (indicated on the left), where SP was incubated with unlabeled PMs (Rx1) in 20 mM Hepes (pH 7.5) and 70 mM KAc buffer for 4 hours at RT and separated over a linear 5 to 20% sucrose gradient. The profiles of the control reactions, where PM, SP, and preassembled dodecameric portal rings were individually incubated in the buffer for 4 hours at RT and separated, are also shown. The black arrow indicates a shift in the portal protein migration down the gradient into higher sucrose concentration toward the position of the preassembled dodecameric portal rings. The black dashed lines indicate the range of fractions where portal oligomers are observed. The green dashed line shows the center of the monomer peak. (**B**) TEMs of negatively stained particles present in fraction 14 (indicated by black arrowhead) from Rx1 (top) and Rx4 (bottom), taken at ×150,000 magnification. Scale bars, 100 nm. Red arrows indicate portal rings that are magnified ×4 and shown in the inset. Scale bars, 20 nm.

such as RNA, cellular crowding, and local critical concentrations of the proteins involved in PC assembly nucleation. However, our data show that P22 portal protein can be coassembled into PC at a single vertex.

Bacteriophage P22 SP facilitates portal ring oligomerization

Previous studies of the portal protein of P22 showed that polymerization of the portal protein monomers into dodecameric rings required incubation for 18 hours at RT and a concentration above 50 mg/ml;

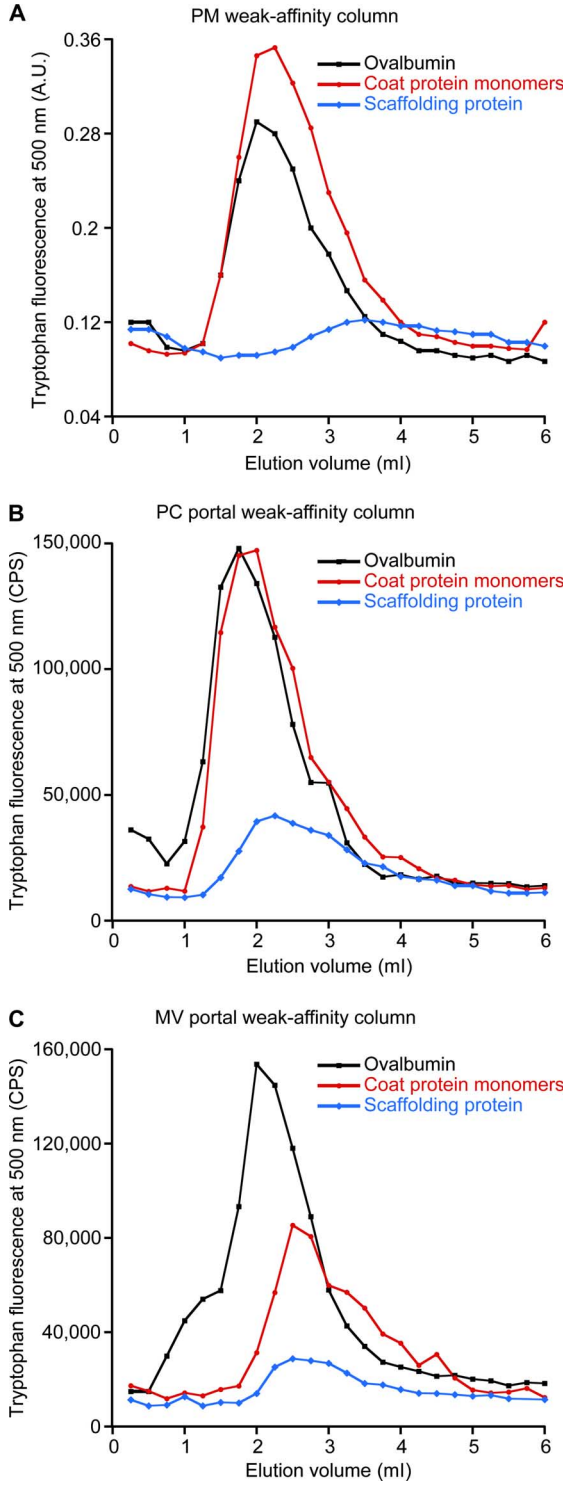

Fig. 8. SP interacts with PMs, not preassembled portal rings (PC portal or MV portal). Elution profile of SP, CP monomers, and ovalbumin from an IMAC bound with His-tagged PMs (**A**) or His-tagged PC portal (**B**) and through an NHS-activated agarose bead column conjugated to non–His-tagged MV portal (**C**). The elution profile of each protein was determined by monitoring intrinsic tryptophan fluorescence of each fraction using AMINCO-Bowman AB2 spectrofluorometer or Horiba FluoroMAX 4 spectrofluorometer at an excitation wavelength at 280 nm, the emission wavelength set to 340 nm, and the bandpasses set to 1 and 8 nm, respectively.

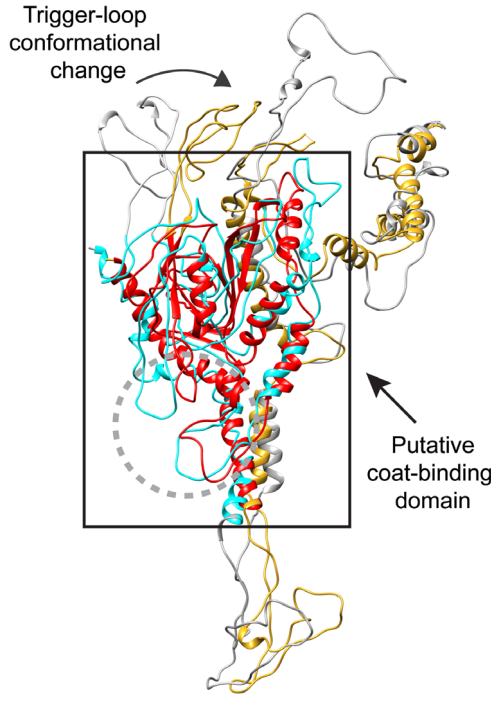

Fig. 9. Structural comparison of the coat-binding region of the PC and MV portal protein structures. Overlay of the PC and MV portal protomers (residues 10 to 599) generated using the program Chimera is presented. The helical barrel domain (residues 600 to 725) is not shown in the overlay. The PC portal protomer is colored gray, with the coat-binding region highlighted in cyan. The MV portal protomer is colored gold, with the coat-binding region highlighted in red. The stem and wing regions that interact with CP in the capsid do not undergo significant conformational transitions between the two portal structures (black box). The regions in the coat binding that undergoes marked conformation change between the two portal structures are highlighted in the gray dashed circle, whereas the black curved arrow points to the major conformational change that occurs in the trigger loop between the two structures.

otherwise, the portal protein primarily remains as metastable monomers (*31*). This observation suggests that, during PC assembly, the polymerization of PMs into dodecamer rings within PCs requires a "triggering" catalyst perhaps absent in vitro. Here, we provide compelling evidence that the trigger is SP. We show that in vitro SP actuates portal ring formation by interaction with PMs (Figs. 6 to 8). We also show that these de novo assembled portal rings are active and are recruited into the growing PC (Fig. 5, B and C, Rx1).

Evidence for portal protein and SP interactions has long been established for bacteriophages Φ29, Mu, T4, SPP1, and lambda, to highlight a few (*30*, *41*–*45*). For instance, the SP of Φ29 was chemically cross-linked to the Φ29 connector protein (portal) at specific interaction sites (*41*). In addition to our study, several lines of evidence have shown that bacteriophage P22 SP plays a key role in the portal protein recruitment and incorporation during PC assembly (*6*, *46*–*48*). Most recently, a cryo-electron microscopy (cryo-EM) structure of P22 PC depicts SP wedged between CP and the portal protein complex (*49*), and an asymmetric reconstruction revealed that the C termini of SP most likely interact with the portal protein complex (*18*). Similarly, for HSV-1, SP aids in the incorporation of the portal protein complex into the growing nascent capsids by forming a scaffold-portal complex (*29*, *50*). Together, these observations support the notion that, in addition to directing capsid assembly, P22's SP also catalyzes the oligomerization of portal rings and its incorporation into PC.

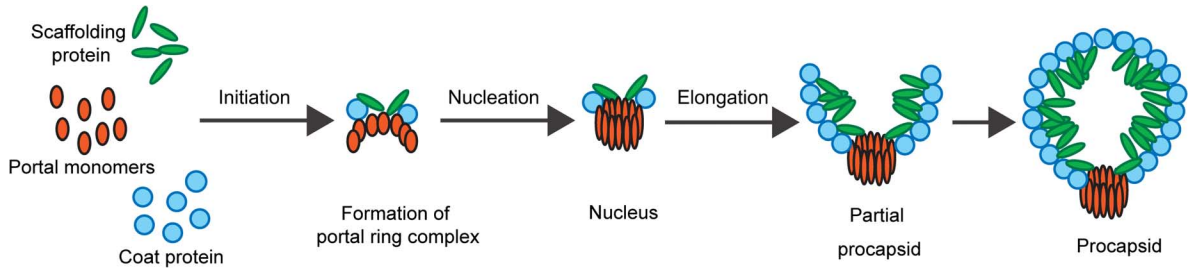

Fig. 10. Proposed model of portal protein incorporation into PCs of bacteriophage P22. Model for the incorporation of portal rings during P22's PC assembly. During initiation of PC assembly, the SP interacts with PMs, instead of interacting exclusively with the CP. The interaction between SP and PM leads to the oligomerization of portal protein monomers into dodecameric rings, which are subsequently incorporated into growing PC head.

In contrast to our hypothesis, a previous study in which portal protein was purified, only PMs were isolated from *Salmonella* cells infected with P22 phage carrying amber (am) mutations in gene 5 (5– *am* N114; codes for CP) and gene 13 (13– *am* H101; blocks cell lysis) (*51*). However, the absence of portal rings in these phage-infected cells can be explained in two ways. First, SP is autogenously regulated, leading to significant down-regulation of protein expression in 5– *am* and 13– *am* phage-infected cells (*52*, *53*). Thus, the very low levels of SP expression in these phage-infected cells could have resulted in negligible nucleation of portal rings from the monomer pool. Second, the authors purified the portal protein monomers using an anion exchange column eluted with a 50 to 300 mM NaCl gradient. However, portal rings elute at much higher salt concentrations (550 to 650 mM), which may also explain their absence in these experiments (*31*).

CP's role in portal incorporation

CP is also likely to be involved in the recruitment of the portal protein complex into PCs. Substituting residue A285 in the accessory I domain of CP sometimes yields $T = 7$ capsid particles containing two portal complexes (*54*, *55*), suggesting the role of I domain in the incorporation of portal protein complex. In addition, the phenotype of the cold-sensitive portal protein mutant (1^{-}*cs* H137) can be suppressed by extragenic second-site mutations within the CP gene, especially in the residues present in the accessory I domain (*28*, *56*). Suppressors of an am mutation of the portal protein (1^{-}*am* H58) have been isolated in the CP gene, and some of these were also found in the I domain (*57*). Thus, these data indicate that the CP interacts with the portal protein, and the accessory I domain of CP probably harbors at least some of the interacting interface of the portal protein. Here, our in vitro assembly experiments have shown that CP also has the ability to bring about the polymerization of PMs into PC assembly–competent portal rings (Fig. 6). Together, all these studies emphasize the fact that there is a cross-talk between the portal protein complex and the CP.

Proposed model of portal protein incorporation into PCs of bacteriophage P22

Our data and the recent cryo-EM reconstructions of bacteriophage P22 PCs (*18*, *49*, *54*) provide evidence for a cross-talk among CP, SP, and the portal protein complex, which we hypothesize is important to direct proper assembly of $T = 7$ PC with only one portal protein complex. We therefore suggest a model for the incorporation of portal rings during P22 PC assembly (Fig. 10), where SP interacts with PM to induce conformational changes in the monomers, hence facilitating the formation of dodecameric portal rings. The assembled portal ring forms a nucleation site, with the chaperone SP directing the addition of the CP subunits around the nucleus, thereby resulting in the formation of a closed icosahedron PC integrated with a portal complex at a sole vertex (Fig. 10). We hypothesize that the portal can act as a "nucleator" of PC assembly by forming a complex with CP and SP, but in its absence, SP and CP still interact to form PLPs. Thus, our model is analogous to that previously proposed for bacteriophage Φ29, where the formation of a connector-SP nucleation complex is essential for incorporation of a single dodecameric connector protein (portal) (*30*, *41*) but expanded to include the novel role of SP in portal ring oligomerization.

In conclusion, we now show that P22's SP can perform yet another role during PC assembly: to orchestrate an intricate, interdependent process of portal protein complex formation via interactions between CP, SP, and portal protein to give rise to perfectly built $T = 7$ icosahedral, functional PCs. Thus, dissecting the structure and function of P22 portal vertex, especially in regard to interactions with SP, will aid us in gaining a better understanding into the mechanism of viral assembly.

MATERIALS AND METHODS

Purification of portal protein

PC portal and MV portal were purified as described (*10*, *17*, *23*). Briefly, to purify and assemble PC portal rings, a full-length His-tagged portal construct was used, and the portal protein was purified by metal-chelating affinity chromatography using High Affinity Ni-NTA Resin (GenScript) and concentrated to ~200 mg/ml using a Millipore-Amicon centrifugal filter device (molecular mass cutoff of 30 kDa). The protein was incubated for 24 hours at RT to promote oligomerization and purified by SEC over a Superose 6 Increase gel filtration column GL 10/300 (GE Healthcare) (*17*). On the other hand, to generate MV portal rings, portal protein was expressed and purified from an untagged full-length portal protein construct, as described (*23*). The purified protein was concentrated to ~200 mg/ml, as above, and incubated for 48 hours at RT to promote oligomerization. The protein was then shifted to 37°C for 3 hours in the presence of 60 mM EDTA and clarified by ultracentrifugation. Finally, the MV portal rings were purified by SEC, as above (*23*).

To purify PMs, plasmid pET21b containing full-length gene 1 (portal protein) (*31*) was transformed into *Escherichia coli* strain BL21 (DE3) cells for expression. The cells were grown at 30°C to mid-log phase in LB medium containing ampicillin (100 μg/ml), induced with 1 mM isopropyl β-D-1-thiogalactopyranoside, and grown for another 5 hours at 28°C. After induction, cells were harvested by sedimentation in a Sorvall SLC-6000 rotor at 5368*g* for 15 min, resuspended in binding buffer [20 mM Hepes (pH 7.5), 500 mM NaCl, and 10 mM imidazole], and frozen at −20°C. The cells were thawed on ice, followed by the addition of phenylmethylsulfonyl fluoride (1 mM), deoxyribonuclease (50 μg/ml), ribonuclease (50 μg/ml), $MgCl_2$ (2 mM), and $CaCl_2$ (0.5 mM), and lysed by sonication at 35 A, 15-s pulse, and 30-s pause, with a total processing time of 3 min using a Misonix Sonicator 4000 with a standard tip. Cell

debris was removed by centrifugation in a Sorvall F18-12 × 50 rotor at 38,725*g* for 15 min. The supernatant was loaded onto a 15-ml Talon Superflow metal affinity resin (Clontech) for purification of the portal protein via the engineered C-terminal hexahistidine (His_6) tag. Unbound protein was eluted with wash buffer [20 mM Hepes (pH 7.5), 500 mM NaCl, and 20 mM imidazole]. The His_6-tagged portal protein was eluted with elution buffer [20 mM Hepes (pH 7.5), 70 mM NaCl, 500 mM imidazole, and 3 mM β-mercaptoethanol] into tubes containing 10 mM EDTA and analyzed by SDS-PAGE. The pooled portal protein was dialyzed twice against portal buffer [20 mm Hepes (pH 7.5), 70 mM NaCl, 3 mM β-mercaptoethanol, and 1 mM EDTA]. Dialyzed PMs were concentrated to approximately 10 mg/ml using a Millipore-Amicon centrifugal filter device (molecular mass cutoff of 30 kDa) at 4°C and were centrifuged for 1 hour at 25,000*g* in Sorvall S120-AT2 rotor to remove aggregates. They were further purified by SEC over a Superose 6 Increase gel filtration column GL 10/300 (GE Healthcare) equilibrated in portal buffer using a BioLogic DuoFlow System (Bio-Rad). Chromatography was carried out at 4°C at a flow rate of 0.25 ml/min. Fractions containing PMs were pooled and concentrated as described above. The Superose 6 Increase column was calibrated using the high- and low-MW standards blue dextran (2000 kDa), thyroglobulin (669 kDa), ferritin (440 kDa), aldolase (158 kDa), ovalbumin (4.4 kDa), and vitamin B_{12} (0.13 kDa) to determine the MWs of PMs.

Labeling of portal protein with AF488 5-SDP ester

Superose 6 Increase column–purified PMs (PM), portal rings (PC and MV portals), or ovalbumin (Sigma-Aldrich) was covalently labeled with AF488 5-SDP ester (Invitrogen Life Technologies) via exposed amine groups. The proteins (~5 mg/ml) were mixed with 0.5 mg of AF488 5-SDP ester resuspended in dimethyl sulfoxide. The reaction was allowed to proceed at RT in darkness for 1 hour for PMs and 3 hours for portal rings and ovalbumin. The reactions were quenched by the addition of 100 μl of 1.5 M hydroxylamine. The excess dye from the AF488-labeled proteins was removed using Zeba Spin Desalting Columns (Thermo Fisher Scientific) equilibrated with portal buffer (as described above). The AF488 PMs, portal rings (AF488 PC portal or AF488 MV portal), or AF488 ovalbumin was centrifuged for 15 min at 25,000*g* in Sorvall S120-AT2 rotor to remove aggregates and was further purified on a Superose 6 Increase column. Peak fractions were pooled and concentrated using a Millipore-Amicon centrifugal filter device (30-kDa cutoff), as described above. Absorbance measurements of the proteins and AF488 5-SDP dye were taken at 280 and 495 nm to determine the corrected protein and incorporated dye concentrations calculated according to the manufacturer's instructions. The labeling efficiency for PMs and portal rings was typically 30 to 35% and for ovalbumin was around 15%.

Charge detection mass spectrometry

CDMS was performed on a home-built instrument. In CDMS, the *m*/*z* and charge of individual ions are measured simultaneously, yielding the mass of each ion (*34*, *35*). Ions were generated by electrospray and transferred through several differentially pumped regions into an electrostatic ion trap. A quadrupole mass filter located before the trap was operated as a high-pass filter that discards ions below an *m*/*z* value determined by the radio frequency applied to the quadrupole mass filter. The ion trap contains a metal tube that the ion passes through each time it oscillates. As the ion passes through the tube, it induces a charge, which is detected by a charge-sensitive preamplifier. The resulting signal was amplified, digitized, and then analyzed with fast Fourier transforms (FFTs). The ion's *m*/*z* was determined from its oscillation frequency, and its charge was determined from the FFT magnitudes. Multiplying the charge and *m*/*z* yields the mass. After 95 ms, the trap was emptied and the trapping cycle was repeated. The instrument and data analysis have previously been described in more detail (*36*).

In vitro assembly reactions

CP monomers were prepared by urea denaturation of empty PC shells. The shells were generated by extraction of SPs from PLPs that contain only the CP and SP, thereby eliminating portal protein, as described previously (*58*). The unfolding reaction of CP monomers was carried out in 6.75 M urea, 20 mM Hepes (pH 7.5) for 30 min at RT and extensively dialyzed against 20 mM Hepes (pH 7.5) at 4°C. Aggregates were removed by ultracentrifugation at 221,121*g* at 4°C for 20 min in a Sorvall S120-AT2 rotor.

SP was purified as previously described (*59*). SP, at a final concentration of 9 μM, was preincubated with AF488 PM or AF488 PC portal or AF488 MV portal or with AF488 ovalbumin at a final concentration of 1.1 μM (in protomer concentration) in 20 mM Hepes (pH 7.5) and 70 mM KAc buffer for up to 4 hours. The assembly reaction was initiated by the addition of refolded CP monomers at a final concentration of 6.4 μM. The reactions were allowed to equilibrate for 4 hours at RT, after which each reaction was applied onto a Superose 6 Increase gel filtration column (GE Healthcare) to separate in vitro assembled PCs from remaining CP, SP, ovalbumin, and labeled portal protein monomers or portal rings. The peak fractions were analyzed by SDS-PAGE. The incorporation of AF488-labeled portal protein or AF488-labeled ovalbumin in these fractions was visualized by PharosFx Plus Molecular Imager (Bio-Rad), and the gel was silver-stained as previously described (*60*). For mock reactions, empty PC shells at 3.2 μM (in protomer concentration) were incubated with AF488 PM or AF488 PC portal or AF488 MV portal or AF488 ovalbumin at a final concentration of 1.1 μM (in protomer concentration) and analyzed as described above.

Immunonegative stain electron microscopy

The antibody labeling of in vitro assembled P22 PCs incorporated with AF488-labeled portal protein was performed as described by Newcomb *et al.* (*61*), with minor modifications. Briefly, 5 μl of the in vitro assembled PC peak fraction, purified from Superose 6 Increase column (refer to Fig. 3, black arrowhead), was absorbed to carbon-coated, 300-mesh copper grid for 2 min at RT. Further steps were performed at RT by floating grids, specimen side down on 100 μl solution drop in a humidified environment. Grids were washed with 0.5× TNE [20 mM tris-HCl (pH 7.5), 0.5 M NaCl, and 1 mM EDTA] and then treated with blocker as described (*61*). Anti-AF488 rabbit immunoglobulin G (IgG) antibody (Invitrogen Life Technologies) was used at a dilution of 1:10 and prepared in 0.5× TNE, and the grids were incubated with the antibody for 1 hour and 30 min. Grids were washed with blocker, as described, to remove excess antibody and then exposed to anti-rabbit IgG (whole-molecule)–gold antibody (10 nm diameter) diluted 1:30 in blocker for 1 hour. The subsequent washing with blocker, 0.5× TNE, and phosphate-buffered saline; fixing (5% glutaraldehyde); and staining (1% uranyl acetate) steps were performed, as previously described (*61*). The grids were viewed in an FEI Tecnai BioTWIN TEM operated at 80 kV and at a nominal magnification of ×68,000. More than 1000 PC particles were analyzed from our assembly and mock reactions with AF488 PC portal or AF488 MV portal. PC particles, where the distance between the center of the gold bead to the nearest PC edge was less than 15 μm, were accounted as PC incorporated with the portal protein.

Sucrose gradient analysis of SP-catalyzed portal rings

Purified SP at a final concentration of 135 μM was preincubated with 16.5 μM PM in 20 mM Hepes (pH 7.5) and 70 mM KAc buffer for 4 hours at RT. After incubation, the reaction was applied to the top of a linear 5 to 20% (w/w) sucrose gradient, prepared using a Gradient Master (model 106, Biocomp Instruments). Gradients were centrifuged at 213,905*g* for 95 min at 20°C in a Sorvall RC-M120EX micro ultracentrifuge in an RP55S rotor. Fractions (100 μl) were collected from the top by using a positive displacement pipetteman. Samples were analyzed by 10% SDS-PAGE and TEM.

For control reactions, SP, at a final concentration of 135 μM, and PM or PC portal, at a final concentration of 16.5 μM, were incubated in 20 mM Hepes buffer (pH 7.5) containing 70 mM KAc for 4 hours at RT and analyzed, as described above.

Negative stain electron microscopy

Electron microscopy samples were prepared by applying 5 μl of fraction 14 from sucrose gradients onto carbon-coated, 400-mesh copper-palladium grids. To make the empty grids, thin carbon films were evaporated onto freshly cleaved mica sheets, floated off onto deionized water, and picked up on 400-mesh copper-palladium grids. Samples were adsorbed for 5 min, washed with water, and stained with 0.75% uranyl formate for 30 s. An FEI Tecnai G2 Spirit BioTWIN TEM equipped with an Advanced Microscopy Techniques 2k XR40 charge-coupled device camera at ×150,000 magnification was used to visualize the grids.

Immobilized PMs or portal rings (PC portal or MV portal) weak-affinity column

To make the weak-affinity column, C-terminal His_6-tagged PMs or PC portal at 2 mg was applied to a 1-ml TALON Superflow and IMAC (Clontech) equilibrated in 20 mM Hepes (pH 7.5) and 70 mM KAc buffer. MV portal (without His_6 tag) at 2 mg was conjugated to NHS-activated agarose slurry (Pierce), as per the manufacturer's instructions. The MV portal–conjugated beads were packed into 1-ml disposable syringe and washed with 20 mM Hepes (pH 7.5) and 70 mM KAc buffer. One hundred microliters of SP or CP was applied onto the columns at 0.2 mg/ml, and 250 μl fractions were collected. Ovalbumin at 0.2 mg/ml was used as a negative control for binding to PM or portal ring (PC portal or MV portal) weak-affinity columns. The tryptophan fluorescence emission of the fractions was measured on an AMINCO-Bowman AB2 spectrofluorometer or Horiba FluoroMAX 4 spectrofluorometer at an excitation wavelength of 295 nm and an emission wavelength of 340 nm, with bandpasses of 1 and 8, respectively. The emitted light in AMINCO-Bowman AB2 fluorometer was recorded in arbitrary units (A.U.), whereas Horiba FluoroMAX 4 spectrometer was measured in counts per second (CPS).

SUPPLEMENTARY MATERIALS

Supplementary material for this article is available at http://advances.sciencemag.org/cgi/content/full/3/7/e1700423/DC1

fig. S1. Analysis of PC and MV portals by native protein gel electrophoresis.

fig. S2. Ovalbumin is not coassembled into PC.

fig. S3. Charge detection mass histogram of SP catalyzed de novo portal rings.

REFERENCES AND NOTES

1. R. W. Hendrix, Symmetry mismatch and DNA packaging in large bacteriophages. *Proc. Natl. Acad. Sci. U.S.A.* **75**, 4779–4783 (1978).
2. S. Casjens, J. King, Virus assembly. *Annu. Rev. Biochem.* **44**, 555–611 (1975).
3. D. L. Caspar, A. Klug, Physical principles in the construction of regular viruses. *Cold Spring Harb. Symp. Quant. Biol.* **27**, 1–24 (1962).
4. C. Bazinet, J. King, The DNA translocating vertex of DSDNA bacteriophage. *Annu. Rev. Microbiol.* **39**, 109–129 (1985).
5. J. M. Valpuesta, J. L. Carrascosa, Structure of viral connectors and their function in bacteriophage assembly and DNA packaging. *Q. Rev. Biophys.* **27**, 107–155 (1994).
6. C. Bazinet, J. King, Initiation of P22 procapsid assembly in vivo. *J. Mol. Biol.* **202**, 77–86 (1988).
7. D. Botstein, C. H. Waddell, J. King, Mechanism of head assembly and DNA encapsulation in Salmonella phage p22. I. Genes, proteins, structures and DNA maturation. *J. Mol. Biol.* **80**, 669–695 (1973).
8. D. Kaiser, M. Syvanen, T. Masuda, DNA packaging steps in bacteriophage lambda head assembly. *J. Mol. Biol.* **91**, 175–186 (1975).
9. A. A. Simpson, Y. Tao, P. G. Leiman, M. O. Badasso, Y. He, P. J. Jardine, N. H. Olson, M. C. Morais, S. Grimes, D. L. Anderson, T. S. Baker, M. G. Rossmann, Structure of the bacteriophage ϕ29 DNA packaging motor. *Nature* **408**, 745–750 (2000).
10. A. S. Olia, P. E. Prevelige Jr., J. E. Johnson, G. Cingolani, Three-dimensional structure of a viral genome-delivery portal vertex. *Nat. Struct. Mol. Biol.* **18**, 597–603 (2011).
11. A. A. Lebedev, M. H. Krause, A. L. Isidro, A. A. Vagin, E. V. Orlova, J. Turner, E. J. Dodson, P. Tavares, A. A. Antson, Structural framework for DNA translocation via the viral portal protein. *EMBO J.* **26**, 1984–1994 (2007).
12. L. Sun, X. Zhang, S. Gao, P. A. Rao, V. Padilla-Sanchez, Z. Chen, S. Sun, Y. Xiang, S. Subramaniam, V. B. Rao, M. G. Rossmann, Cryo-EM structure of the bacteriophage T4 portal protein assembly at near-atomic resolution. *Nat. Commun.* **6**, 7548 (2015).
13. R. H. Rochat, X. Liu, K. Murata, K. Nagayama, F. J. Rixon, W. Chiu, Seeing the portal in herpes simplex virus type 1 B capsids. *J. Virol.* **85**, 1871–1874 (2011).
14. J. C. Brown, W. W. Newcomb, Herpesvirus capsid assembly: Insights from structural analysis. *Curr. Opin. Virol.* **1**, 142–149 (2011).
15. G. Cardone, D. C. Winkler, B. L. Trus, N. Cheng, J. E. Heuser, W. W. Newcomb, J. C. Brown, A. C. Steven, Visualization of the herpes simplex virus portal in situ by cryo-electron tomography. *Virology* **361**, 426–434 (2007).
16. B. L. Trus, N. Cheng, W. W. Newcomb, F. L. Homa, J. C. Brown, A. C. Steven, Structure and polymorphism of the UL6 portal protein of herpes simplex virus type 1. *J. Virol.* **78**, 12668–12671 (2004).
17. R. K. Lokareddy, R. S. Sankhala, A. Roy, P. V. Afonine, T. Motwani, C. M. Teschke, K. N. Parent, G. Cingolani, Portal protein functions akin to a DNA-sensor that couples genome-packaging to icosahedral capsid maturation. *Nat. Commun.* **8**, 14310 (2017).
18. J. Tang, G. C. Lander, A. Olia, R. Li, S. Casjens, P. Prevelige Jr., G. Cingolani, T. S. Baker, J. E. Johnson, Peering down the barrel of a bacteriophage portal: The genome packaging and release valve in p22. *Structure* **19**, 496–502 (2011).
19. C. M. Teschke, K. N. Parent, 'Let the phage do the work': Using the phage P22 coat protein structures as a framework to understand its folding and assembly mutants. *Virology* **401**, 119–130 (2010).
20. J. King, D. Botstein, S. Casjens, W. Earnshaw, S. Harrison, E. Lenk, Structure and assembly of the capsid of bacteriophage P22. *Philos. Trans. R. Soc. Lond. Biol. Sci.* **276**, 37–49 (1976).
21. P. E. Prevelige Jr., J. King, Assembly of bacteriophage P22: A model for ds-DNA virus assembly. *Prog. Med. Virol.* **40**, 206–221 (1993).
22. V. Israel, E proteins of bacteriophage P22. I. Identification and ejection from wild-type and defective particles. *J. Virol.* **23**, 91–97 (1977).
23. K. Lorenzen, A. S. Olia, C. Uetrecht, G. Cingolani, A. J. R. Heck, Determination of stoichiometry and conformational changes in the first step of the P22 tail assembly. *J. Mol. Biol.* **379**, 385–396 (2008).
24. S. Casjens, J. King, P22 morphogenesis. I: Catalytic scaffolding protein in capsid assembly. *J. Supramol. Struct.* **2**, 202–224 (1974).
25. H. Murialdo, A. Becker, Head morphogenesis of complex double-stranded deoxyribonucleic acid bacteriophages. *Microbiol. Rev.* **42**, 529–576 (1978).
26. M. E. Cerritelli, F. W. Studier, Assembly of T7 capsids from independently expressed and purified head protein and scaffolding protein. *J. Mol. Biol.* **258**, 286–298 (1996).
27. S. D. Moore, P. E. Prevelige Jr., Bacteriophage p22 portal vertex formation in vivo. *J. Mol. Biol.* **315**, 975–994 (2002).
28. C. Bazinet, R. Villafane, J. King, Novel second-site suppression of a cold-sensitive defect in phage P22 procapsid assembly. *J. Mol. Biol.* **216**, 701–716 (1990).
29. W. W. Newcomb, F. L. Homa, J. C. Brown, Involvement of the portal at an early step in herpes simplex virus capsid assembly. *J. Virol.* **79**, 10540–10546 (2005).
30. C.-y. Fu, P. E. Prevelige Jr., In vitro incorporation of the phage Phi29 connector complex. *Virology* **394**, 149–153 (2009).
31. S. D. Moore, P. E. Prevelige Jr., Structural transformations accompanying the assembly of bacteriophage P22 portal protein rings in vitro. *J. Biol. Chem.* **276**, 6779–6788 (2001).
32. G. Cingolani, S. D. Moore, P. E. Prevelige Jr., J. E. Johnson, Preliminary crystallographic analysis of the bacteriophage P22 portal protein. *J. Struct. Biol.* **139**, 46–54 (2002).
33. A. Poliakov, E. van Duijn, G. Lander, C.-y. Fu, J. E. Johnson, P. E. Prevelige Jr., A. J. R. Heck, Macromolecular mass spectrometry and electron microscopy as complementary tools for investigation of the heterogeneity of bacteriophage portal assemblies. *J. Struct. Biol.* **157**, 371–383 (2007).

34. S. D. Fuerstenau, W. H. Benner, Molecular weight determination of megadalton DNA electrospray ions using charge detection time-of-flight mass spectrometry. *Rapid Commun. Mass Spectrom.* **9**, 1528–1538 (1995).
35. N. C. Contino, E. E. Pierson, D. Z. Keifer, M. F. Jarrold, Charge detection mass spectrometry with resolved charge states. *J. Am. Soc. Mass Spectrom.* **24**, 101–108 (2013).
36. D. Z. Keifer, D. L. Shinholt, M. F. Jarrold, Charge detection mass spectrometry with almost perfect charge accuracy. *Anal. Chem.* **87**, 10330–10337 (2015).
37. P. E. Prevelige Jr., D. Thomas, J. King, Nucleation and growth phases in the polymerization of coat and scaffolding subunits into icosahedral procapsid shells. *Biophys. J.* **64**, 824–835 (1993).
38. A. R. Poteete, V. Jarvik, D. Botstein, Encapsulation of phage P22 DNA in vitro. *Virology* **95**, 550–564 (1979).
39. D. Zopf, S. Ohlson, Weak-affinity chromatography. *Nature* **346**, 87–88 (1990).
40. M. M. Suhanovsky, K. N. Parent, S. E. Dunn, T. S. Baker, C. M. Teschke, Determinants of bacteriophage P22 polyhead formation: The role of coat protein flexibility in conformational switching. *Mol. Microbiol.* **77**, 1568–1582 (2010).
41. C.-y. Fu, C. Uetrecht, S. Kang, M. C. Morais, A. J. Heck, M. R. Walter, P. E. Prevelige Jr., A docking model based on mass spectrometric and biochemical data describes phage packaging motor incorporation. *Mol. Cell. Proteomics* **9**, 1764–1773 (2010).
42. H. Murialdo, A. Becker, A genetic analysis of bacteriophage lambda prohead assembly in vitro. *J. Mol. Biol.* **125**, 57–74 (1978).
43. R. Grimaud, Bacteriophage Mu head assembly. *Virology* **217**, 200–210 (1996).
44. N. L. Yap, V. B. Rao, Novel mutants in the 5′ upstream region of the portal protein gene 20 overcome a gp40-dependent prohead assembly block in bacteriophage T4. *J. Mol. Biol.* **263**, 539–550 (1996).
45. A. Dröge, M. A. Santos, A. C. Stiege, J. C. Alonso, R. Lurz, T. A. Trautner, P. Tavares, Shape and DNA packaging activity of bacteriophage SPP1 procapsid: Protein components and interactions during assembly. *J. Mol. Biol.* **296**, 117–132 (2000).
46. W. Earnshaw, J. King, Structure of phage P22 coat protein aggregates formed in the absence of the scaffolding protein. *J. Mol. Biol.* **126**, 721–747 (1978).
47. B. Greene, J. King, Scaffolding mutants identifying domains required for P22 procapsid assembly and maturation. *Virology* **225**, 82–96 (1996).
48. P. R. Weigele, L. Sampson, D. Winn-Stapley, S. R. Casjens, Molecular genetics of bacteriophage P22 scaffolding protein's functional domains. *J. Mol. Biol.* **348**, 831–844 (2005).
49. D.-H. Chen, M. L. Baker, C. F. Hryc, F. DiMaio, J. Jakana, W. Wu, M. Dougherty, C. Haase-Pettingell, M. F. Schmid, W. Jiang, D. Baker, J. A. King, W. Chiu, Structural basis for scaffolding-mediated assembly and maturation of a dsDNA virus. *Proc. Natl. Acad. Sci. U.S.A.* **108**, 1355–1360 (2011).
50. W. W. Newcomb, D. R. Thomsen, F. L. Homa, J. C. Brown, Assembly of the herpes simplex virus capsid: Identification of soluble scaffold-portal complexes and their role in formation of portal-containing capsids. *J. Virol.* **77**, 9862–9871 (2003).
51. C. Bazinet, J. Benbasat, J. King, J. M. Carazo, J. L. Carrascosa, Purification and organization of the gene 1 portal protein required for phage P22 DNA packaging. *Biochemistry* **27**, 1849–1856 (1988).
52. S. Casjens, M. B. Adams, Posttranscriptional modulation of bacteriophage P22 scaffolding protein gene expression. *J. Virol.* **53**, 185–191 (1985).
53. E. Wyckoff, S. Casjens, Autoregulation of the bacteriophage P22 scaffolding protein gene. *J. Virol.* **53**, 192–197 (1985).
54. A. A. Rizzo, M. M. Suhanovsky, M. L. Baker, L. C. R. Fraser, L. M. Jones, D. L. Rempel, M. L. Gross, W. Chiu, A. T. Alexandrescu, C. M. Teschke, Multiple functional roles of the accessory I-domain of bacteriophage P22 coat protein revealed by NMR structure and CryoEM modeling. *Structure* **22**, 830–841 (2014).
55. M. M. Suhanovsky, C. M. Teschke, Bacteriophage P22 capsid size determination: Roles for the coat protein telokin-like domain and the scaffolding protein amino-terminus. *Virology* **417**, 418–429 (2011).
56. C. L. Gordon, J. King, Temperature-sensitive mutations in the phage P22 coat protein which interfere with polypeptide chain folding. *J. Biol. Chem.* **268**, 9358–9368 (1993).
57. J. Jarvik, D. Botstein, Conditional-lethal mutations that suppress genetic defects in morphogenesis by altering structural proteins. *Proc. Natl. Acad. Sci. U.S.A.* **72**, 2738–2742 (1975).
58. E. Anderson, C. M. Teschke, Folding of phage P22 coat protein monomers: Kinetic and thermodynamic properties. *Virology* **313**, 184–197 (2003).
59. P. E. Prevelige Jr., D. Thomas, J. King, Scaffolding protein regulates the polymerization of P22 coat subunits into icosahedral shells in vitro. *J. Mol. Biol.* **202**, 743–757 (1988).
60. T. Rabilloud, G. Carpentier, P. Tarroux, Improvement and simplification of low-background silver staining of proteins by using sodium dithionite. *Electrophoresis* **9**, 288–291 (1988).
61. W. W. Newcomb, R. M. Juhas, D. R. Thomsen, F. L. Homa, A. D. Burch, S. K. Weller, J. C. Brown, The UL6 gene product forms the portal for entry of DNA into the herpes simplex virus capsid. *J. Virol.* **75**, 10923–10932 (2001).

Acknowledgments: We thank M. Cantino, S. Daniels, and X. Sun of University of Connecticut Bioscience Electron Microscopy Laboratory for assistance with TEM. We also thank C. Dedeo and M. Siegel for their contributions and M. Suhanovsky and K. Asija for their comments on this manuscript. **Funding:** This work was supported by NSF grant CHE-1531823 (to M.F.J.) and NIH grants GM100888 (to G.C.) and GM076661 (to C.M.T.). **Author contributions:** T.M. performed most of the experiments and wrote the paper with C.M.T. R.K.L. purified the PC portal and MV portal proteins. C.A.D. and M.F.J. determined the oligomeric state of the portal protein by CDMS. J.R.C. established the conditions for ring incorporation during in vitro PC assembly. All authors contributed to the writing and editing of the manuscript. **Competing interests:** The authors declare that they have no competing interests. **Data and materials availability:** All data needed to evaluate the conclusions in the paper are present in the paper and/or the Supplementary Materials. Additional data related to this paper may be requested from the authors.

Submitted 8 February 2017
Accepted 19 June 2017
Published 26 July 2017
10.1126/sciadv.1700423

Citation: T. Motwani, R. K. Lokareddy, C. A. Dunbar, J. R. Cortines, M. F. Jarrold, G. Cingolani, C. M. Teschke, A viral scaffolding protein triggers portal ring oligomerization and incorporation during procapsid assembly. *Sci. Adv.* **3**, e1700423 (2017).